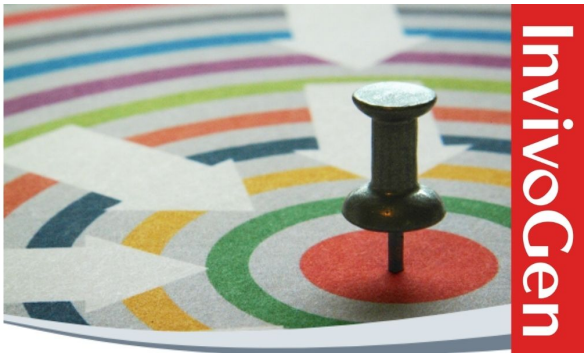

The Journal of Immunology
RESEARCH ARTICLE | AUGUST 15 2005

Activation of Thymic Regeneration in Mice and Humans following Androgen Blockade FREE

Jayne S. Sutherland; ... et. al

J Immunol (2005) 175 (4): 2741–2753.
https://doi.org/10.4049/jimmunol.175.4.2741

Activation of Thymic Regeneration in Mice and Humans following Androgen Blockade

Jayne S. Sutherland,[1]* Gabrielle L. Goldberg,[2]* Maree V. Hammett,[2]* Adam P. Uldrich,[3]* Stuart P. Berzins,[†] Tracy S. Heng,[2]* Bruce R. Blazar,[‡] Jeremy L. Millar,[§] Mark A. Malin,[2]* Ann P. Chidgey,[2]* and Richard L. Boyd[2]*

The thymus undergoes age-related atrophy, coincident with increased circulating sex steroids from puberty. The impact of thymic atrophy is most profound in clinical conditions that cause a severe loss in peripheral T cells with the ability to regenerate adequate numbers of naive CD4$^+$ T cells indirectly correlating with patient age. The present study demonstrates that androgen ablation results in the complete regeneration of the aged male mouse thymus, restoration of peripheral T cell phenotype and function and enhanced thymus regeneration following bone marrow transplantation. Importantly, this technique is also applicable to humans, with analysis of elderly males undergoing sex steroid ablation therapy for prostatic carcinoma, demonstrating an increase in circulating T cell numbers, particularly naive (TREC$^+$) T cells. Collectively these studies represent a fundamentally new approach to treating immunodeficiency states in humans. *The Journal of Immunology,* **2005, 175: 2741–2753.**

The thymus is critical for establishing and maintaining the peripheral T cell pool. It does so in the young by exporting precisely controlled levels of naive CD4$^+$ and CD8$^+$ T cells, termed recent thymic emigrants (RTE)[4] (1). This results in a diverse peripheral TCR repertoire, essential for an effective immune response against a broad range of invading pathogens. Paradoxically, however, the thymus undergoes progressive decline in its structure and function with age, coinciding with an increase in circulating sex steroid levels from puberty (2, 3). Indeed, the suppressive influence of sex steroids on the thymus is so profound, that surgical or chemical (via luteinizing hormone-releasing hormone (LHRH) analogues) castration can reverse thymus atrophy in both males and females (4, 5), while the readministration of sex steroids inhibits this thymus regeneration (6, 7). The direct consequence of age-associated thymic atrophy is a reduction in the export of naive T cells (1, 8) and a homeostatic compensatory increase in the memory T cell population resulting in detrimental changes within the peripheral T cell pool. Specifically, T cell-dependent Ab formation (9), the generation of allospecific cytolytic T cells (10), and T cell responses to mitogen or Ag stimulation (11) are all decreased with age. Due to the complex symbiosis that exists between the thymic epithelium and developing thymocytes (12), the precise mechanism(s) underlying thymus atrophy are still unclear. Defects with age have been seen at the level of the bone marrow (BM) hemopoietic stem cells (HSC) (13–15), the intrathymic T cell progenitors (16), and the thymic epithelium (17, 18). The kinetics of these defects are difficult to determine; thus, any method of thymic regeneration must consider all these factors.

Although the loss of thymic function with age does not immediately translate to major clinical problems, the implications of defective thymopoiesis become paramount when regeneration of the peripheral T cell pool is required following destruction of the immune system in many clinical settings. The most precise technique to date for analysis of thymic function in humans is through measurement of TCR excision circles (TRECs) in the peripheral blood. Although persistent thymus function is evident with age (19, 20), there is a profound decrease in TREC levels (thymic output) (21). Not surprisingly adults, who display only low levels of thymic export (8), show a marked delay in peripheral T cell pool regeneration and a far greater incidence of opportunistic infections compared with their younger counterparts whose thymus may be as much as 10 times more effective (22). In addition, there is a strong inverse correlation between age and the recovery of phenotypically naive T cells and TREC levels following chemotherapy and BM transplantation (BMT) and reduction of viral load in HIV$^+$ patients (21–24). Thus, a mechanism that would enhance thymus regeneration in immunosuppressed and/or aged individuals would be of significant clinical value.

A recent study demonstrated an increase in T cell levels and responses following androgen deprivation in young mice (25). In the present study, we show complete restoration of the very old (18–24 mo) mouse thymic structure (both epithelial and lymphocytic) and function with castration, resulting in normalization of T cell defects in the peripheral lymphoid organs. This enhanced thymus function was not limited to the aged but was also induced in young adult mice (3 mo), which had undergone BMT following either surgical or chemical castration. Importantly, this involved increased levels of Lin$^-$Sca-1$^+$c-*kit*$^+$ (LSK) in the BM and their intrathymic conversion into dendritic cells (DC) and T cells as

*Department of Immunology, Monash University Medical School, Prahran, Victoria, Australia; †Department of Microbiology and Immunology, University of Melbourne, Melbourne, Victoria, Australia; ‡Division of Bone Marrow Transplantation, University of Minnesota, Minneapolis, MN 55455; and §Department of Radiation Oncology, William Buckland Radiotherapy Centre, Prahran, Victoria, Australia

Received for publication January 11, 2005. Accepted for publication June 8, 2005.

The costs of publication of this article were defrayed in part by the payment of page charges. This article must therefore be hereby marked *advertisement* in accordance with 18 U.S.C. Section 1734 solely to indicate this fact.

[1] Address correspondence and reprint requests to Dr. Jayne S. Sutherland at the current address: Transplant Immunobiology Group, Anthony Nolan Research Institute, Royal Free Hospital, London NW3 2QG, U.K. E-mail address: j.sutherland@medsch.ucl.ac.uk

[2] Current address: Monash Immunology and Stem Cell Laboratories, Monash University, Wellington Road, Clayton, Victoria, Australia.

[3] Current address: University of Melbourne, Melbourne, Victoria, Australia.

[4] Abbreviations used in this paper: RTE, recent thymic emigrant; LHRH, luteinising hormone-releasing hormone; BM, bone marrow; HSC, hemopoietic stem cell; TREC, TCR excision circle; BMT, bone marrow transplantation; LSK, Lin-Sca-1$^+$c-*kit*$^+$; LHRH-A, LHRH agonist; DC, dendritic cell; TN, triple negative; PFA, paraformaldehyde; MTS, mouse thymic stromal; HPRT, hypoxanthine phosphoribosyltransferase; ECM, extracellular matrix; Fgf, fibroblast growth factor.

0022-1767/05/$02.00

occurs normally. We have also attempted to determine the mechanism of the profound effect of androgen withdrawal. Interestingly, while sex steroid ablation resulted in major changes within the thymic microenvironment, molecular profiling indicated no significant changes in IL-7, TGF-β, and fibroblast growth factor (Fgf)7 mRNA within total thymic stroma; all of which have been shown to modulate thymic growth in other systems.

We have also shown this treatment is applicable to elderly humans, with analysis of the peripheral blood of prostate cancer patients undergoing sex steroid ablation therapy, demonstrating a significant increase in T cell numbers. Reactivation of the thymic-dependent T cell pathway in these patients was demonstrated by an increase in naive $CD4^+TREC^+$ cells by 4 mo of LHRH agonist (LHRH-A) treatment.

Materials and Methods

Surgical castration

Mice were anesthetized and a small scrotal incision made to reveal the testes. These were sutured and removed along with surrounding fatty tissue. The wound was closed using surgical staples. Sham-castration followed the above procedure without removal of the testes and was used as controls for all studies.

Chemical castration

Mice were injected i.m. with a 3-mo depot preparation of LHRH-A at a dose of either 0.4 or 1.2 mg 2 wk before BMT. Control mice were injected with PBS.

BM reconstitution

For surgical castration experiments, recipient mice (3- to 4-mo-old C57BL/6J) were subjected to 5.5 Gy irradiation twice over a 3-h interval. One hour following the second irradiation dose, mice were injected i.v. with 5×10^6 donor BM cells. BM was obtained by passing RPMI 1640 through the tibias and femurs of donor (2-mo-old congenic C57BL/6J $Ly5.1^+$) mice. For chemical castration experiments, an allogeneic model was used. C57BL/6J recipients (6–8 wk) were subjected to 9 Gy of irradiation. Donor BM was obtained from BALB/c mice, pan-T cell-depleted and 10^7 cells administered via i.v. injection.

HSV-1 immunization

Following anesthetic, mice were injected in the foot-hock with 4×10^5 PFU of HSV-1 in sterile PBS. Analysis of the draining (popliteal) lymph nodes was performed on D5 postinfection.

BrdU incorporation

Mice received two i.p. injections of BrdU (Sigma-Aldrich) at a dose of 100 mg/kg body weight in 100 μl of PBS, 4 h apart. Control mice received vehicle alone injections.

Analysis of RTE

FITC labeling of thymocytes was performed as described previously (8). Quantification of RTE populations and daily export rates were performed as described previously (1).

Flow cytometry

Predominantly, cells were labeled with anti-$\alpha\beta$TCR-FITC, anti-CD4-PE, and anti-CD8-allophycocyanin. For RTE analysis, cells were labeled with CD44-biotin, CD4-PE, and CD8-PerCP. For HSV-1 studies, popliteal lymph node cells were stained for anti-CD25-PE, anti-CD8-APC, and anti-Vβ10-biotin. For detection of DC, a FcR block was used before staining for CD45.1-FITC, $I\text{-}A^b$-PE, and CD11c-biotin. For detection of LSK, BM cells were gated on Lin^- cells by collectively staining with anti-CD3, -CD4, -CD8, -Gr-1, -B220, and -Mac-1 (all conjugated to FITC). LSK were detected by staining with CD117-APC and Sca-1-PE. For triple negative (TN) thymocyte analysis, cells were gated on the Lin^- population and detected by staining with CD44-biotin, CD25-PE, and c-*kit*-APC. For BrdU analysis, cells were surface labeled with anti-CD4-PE and anti-CD8-APC followed by fixation in 1% paraformaldehyde (PFA). Washed cells were incubated in 500 μl of DNase (100 Kunitz units) (Roche) for 30 min at 37°C. Finally, cells were incubated with anti-BrdU-FITC (BD Biosciences) for 30 min at room temperature, washed, and resuspended for FACS analysis. For BrdU analysis of TN subsets, cells were collectively gated out on Lin^- cells in allophycocyanin, followed by detection for CD44-biotin and CD25-PE before BrdU detection. For analysis of apoptosis, thymocytes were stained for CD4-PE, CD8-allophycocyanin, $\alpha\beta$TCR-FITC, and Annexin V-biotin. Positive controls were cells cultured overnight (37°C, 5% CO_2) either alone or in combination with Con A. All biotinylated Abs were detected with streptavidin-PerCP, except for CD44-biotin used in RTE analysis, which was detected with streptavidin-allophycocyanin. All Abs were obtained from BD Pharmingen.

Immunofluorescence

Frozen sections (4–10 μm) were cut using a Tissue-Tek II cryostat (Miles Scientific). For analysis of mouse thymic stromal (MTS) Abs, sections were labeled with MTS6, MTS15, MTS16, and MTS24. All primary Abs were developed in this laboratory. Abs were detected with anti-rat-FITC (QXF; Sigma-Aldrich). For BrdU detection, sections were fixed in 100% acetone and surface labeled with anti-cytokeratin (DakoCytomation), followed by detection with anti-ratCy3 (Molecular Probes). Sections were then incubated for 30 min in 70% ethanol, followed by an additional 30 min in 4 M HCl. Neutralization was performed using 1 M sodium borate buffer (Sigma-Aldrich) for 5 min, followed by two washes in PBS. A final incubation with anti-BrdU-FITC was then performed for 30 min at room temperature.

Molecular analysis of thymic tissue

Preparation of thymic tissue. Nine- to 12-mo-old C57BL/6J mice were surgically castrated or sham castrated ($n = 10$) and thymii were removed at days 1, 2, 4, 7, or 10 postsurgery. For stromal cell preparations, thymii were digested as described previously (26). Briefly, they were enzymatically digested in 0.125% (w/v) collagenase D (Roche Applied Sciences) or trypsin (Sigma-Aldrich) in the case of the final fraction and 0.1% (w/v) DNase (Roche Applied Sciences) in RPMI 1640. To isolate the stromal cell population, cells were incubated with CD45 microbeads and depleted of $CD45^+$ cells using an autoMACS (Miltenyi Biotec). For thymocyte suspensions, cells were isolated by gently teasing out cells into RPMI 1640.

Total RNA was isolated using Tri-Reagent (Molecular Research Center), according to the manufacturer's instructions.

Semiquantitative and quantitative PCR analysis. Total RNA from $CD45^-$ thymic stromal cells and thymocytes was reverse transcribed using Superscript II reverse transcriptase (Invitrogen Life Technologies), according to the manufacturer's protocol. For semiquantitative RT-PCR, cDNA in three serial dilutions were PCR amplified for 33 and 35 cycles with PCR Master Mix (Promega). PCR cycling conditions for Fgf7 and FgfR2IIIB primers were 94°C for 40 s, 60°C for 40 s, 72°C for 40 s, followed by a 72°C, 5-min extension. PCR products were quantified with LabWorks software. Real-time quantitative PCR was performed on a Corbett Rotor-Gene 3000 (Corbett Research) using heat-activated SYBR Green Supermix (Invitrogen Life Technologies). After an initial hold of 2 min at 94°C, the samples were cycled at 94°C for 30s, 56°C for 30s, 72°C for 90 s, followed by a 72°C, 5-min extension.

All cDNA templates were standardized for hypoxanthine phosphoribosyltransferase (HPRT) expression to correct for variations in RNA concentration. The primer sequences (GeneWorks) used were as follows: HPRT, forward, 5′-CACAGGACTAGAACACCTGC-3′, and reverse, 5′-GCTGGTGAAAAGGACCTCT-3′; IL-7, forward, 5′-TATTCTAGAATGTTCCATGTTTCTTTTAGA-3′, and reverse, 5′-CTTTTTCTGTTCCTTTA-3′; Fgf7, forward, 5′-GCCTTGTCACGACCTGTTTC-3′, and reverse, 5′-AGTTCACACTCGTAGCCGTTTG-3′; TGF-β1, forward, 5′-CTACTGCTTCAGCTCCACAG-3′, and reverse, 5′ TGCACTTGCAGGAGCGCAC 3′; IL7Rα, forward, 5′-TTACTTCAAAGGCTTCTGGAG-3′, and reverse, 5′-CTGGCTTCAACGCCTTTCACCTCA-3′; FgfR2IIIb, forward, 5′-TGCCGCCAACACTGTGAAGTTC-3′, and reverse, 5′-TCAACGACATCCAGGTGGTAGG-3′; and TGFβRII, forward, 5′-ACTTGACCTGTTGCCTGTGTGAC-3′, and reverse, 5′-CTGGCTTCAACGCCTTTCACCTCA-3′.

T lymphocyte stimulation assay. For TCR-specific stimulation, spleen cells were incubated for 48 h on plates previously coated with purified anti-CD3 (1–10 μg/ml) alone or costimulated with anti-CD28 (10 μg/ml) (BD Pharmingen). Following plaque formation (48–72 h), 1 μCi of [^{3}H]thymidine was added to each well, and plates were incubated for an additional 16–24 h. Plates were harvested onto filter mats, and incorporation of [^{3}H]thymidine was determined using liquid scintillation on a beta counter (Packard-Coulter). All samples had similar proportion/number of total T cells (as assessed by flow cytometry).

Cytotoxicity assay of lymph node cells. Lymph node cells were incubated for 3 days at 37°C, 6.5% CO_2. Specificity was determined using a non-transfected cell line (EL4) pulsed with $gB_{498\text{-}505}$ peptide and EL4 cells

alone as a control. A starting E:T ratio of 30:1 was used. The plates were incubated at 37°C, 6.5% CO_2 for 4 h and then centrifuged 650_{gmax} for 5 min. Supernatant (100 μl) was harvested from each well and transferred into glass fermentation tubes for measurement by a Packard Cobra autogamma counter.

Human studies

Patients. Sixteen patients with clinical tumor-node-metastasis stage I–III prostate cancer were chosen for analysis. All subjects were males aged between 60 and 77 years who underwent standard combined androgen blockade based on LHRH-A treatment before localized radiation therapy for prostate cancer. Ethics approval was obtained from The Alfred Hospital Committee for Ethical Research on Humans (trial number 106/99).

FACS analysis. The appropriate Ab mixture (20 μl) was added to 200 μl of whole blood and incubated in the dark at room temperature for 30 min. For removal of RBC, 2 ml of FACS lysis buffer (BD Biosciences) was then added to each tube, vortexed, and incubated for 10 min at room temperature in the dark. Samples were centrifuged at 600_{gmax}; supernatant was removed, and cells washed twice in PBS/FCS/Az. Finally, cells were resuspended in 1% PFA for FACS analysis. Samples were stained with Abs to CD19-FITC, CD4-FITC, CD8-APC, CD27-FITC, CD45RA-PE, CD45RO-CyChrome, CD62L-FITC, and CD56-PE (all from BD Pharmingen).

Ki-67 Ag analysis. For detection of proliferating cells, samples were surface stained with CD27-FITC, CD45RO-CyChrome, and $CD4^-$ or CD8-allophycocyanin (BD Pharmingen). Following red cell lysis, samples were incubated for 20 min at room temperature in the dark in 500 μl of FACS permeabilizing solution (BD Biosciences). Washed samples (2 ml of FACS buffer, 5 min, 600_{gmax}, room temperature) were incubated with anti-Ki67-PE (or the appropriate isotype control) (BD Pharmingen) for 30 min at room temperature in the dark. Samples were then washed and resuspended in 1% PFA for analysis.

TREC analysis

Cell sorting. PBMC were incubated with anti-CD4-FITC and anti-CD8-allophycocyanin for 30 min on ice, washed (2 ml of FACS buffer), and fixed by the dropwise addition of 1 ml of 3% formalin in PBS (with agitation). Samples were incubated for an additional 30 min, washed, and resuspended in 500 μl of FACS buffer for sorting. Cells were sorted into $CD4^+$ and $CD8^+$ populations on a MoFLO (DakoCytomation).

DNA isolation. Cells were sorted directly into PCR grade 0.5-ml Eppendorf tubes, centrifuged (8 min, 2500_{gmax}), and resuspended in proteinase K (Boehringer Mannheim) digestion buffer (2×10^5 cells/20 μl of a 0.8 mg/ml solution). Samples were incubated for 1 h at 56°C, followed by 10 min at 95°C to inactivate the proteinase.

Real-time PCR using molecular beacons. Real-time PCR for analysis of TREC content in sorted cells was performed as described previously (27). Each 50-μl reaction contained 5 μl of DNA, and the final concentration of each component was as follows: 1× Taqman buffer A, 3.5 mM $MgCl_2$, 0.4pmol/μl of each primer, and 1.25 U of AmpliTaq Gold DNA polymerase. The primers were sense, 5′-GGATGGAAAACACAGTGTGACA TGG-3′, and antisense, 5′-CTGTCAACAAAGGTGATGCCACATCC-3′. One cycle of denaturation (95°C for 10 min) was performed, followed by 45 cycles of amplification (94°C for 30 s, 60°C for 30 s, and 72°C for 30 s). To normalize for cell equivalents in the input DNA, a separate real-time PCR assay was used to quantify the CCR5-coding sequence, which contains no pseudogenes. TREC frequency (expressed as TREC per 10^5 cells) was used to calculate the total number of TREC in a given population by multiplying by the number of cells ($\times 10^5$ $CD4^+$ or $CD8^+$) per ml blood. Where possible, analysis was performed in duplicate (dependent on cell number).

Statistical analysis. Statistical analysis was performed using Instat II software. For mouse studies, a Mann-Whitney *U* test was performed. For human studies, each patient acted as an internal control by comparing pre- and posttreatment results and were analyzed using paired Student's *t* tests or Wilcoxon signed rank tests.

Results

The aged thymus contains all stromal and T cell subsets but has limited functional capacity

Analysis of the thymic macro- and microenvironments revealed distinct changes with age: the aged (24 mo) thymus was markedly smaller in size compared with the young adult (2 mo) thymus (Fig. 1*a*). Furthermore, there was a severe disruption to the thymic microenvironment, predominantly a collapse of the cortical epithelium with loss of a distinct corticomedullary junction (Fig. 1*b*). However, the aged mouse thymus was clearly capable of thymopoiesis, with all the major CD4, CD8, and $\alpha\beta$TCR-defined (data not shown) T cell subsets in similar proportions to the young adult thymus (Fig. 1*c*).

Further analysis of the thymic microenvironment revealed a decreased expression of MHC class II (detected by mAb, MTS6; Fig. 1*d*) with age. Conversely, the aged (2 year) thymus showed enhanced expression of mAb MTS15 (26), identifying fibroblasts associated with the vasculature and also of extracellular matrix (ECM) proteins (detected by mAb, MTS16). In addition, expression of MTS24, which detects a subset of thymic epithelium containing progenitor capacity for the thymic microenvironment (28), was also proportionally enhanced with age (Fig. 1*d*).

Castration completely reverses thymic atrophy and restores thymic architecture

Following surgical castration of aged mice, a rapid regeneration of the thymus was evident both at the gross morphological (Fig. 1*a*) and histological levels (Fig. 1*b*). Interestingly, despite the dramatic changes occurring postcastration, proportions of the major thymocyte subsets remained constant at all time points analyzed, indicating a synchronous expansion (Fig. 1*c*). Associated with this was a normalization of the thymic microenvironment into clearly defined cortical and medullary regions (Fig. 1*b*). The enhanced expression of MTS15 and MTS16 with age was even more striking at 2 wk postcastration together with a profound increase in expression of MHC class II (Fig. 1*d*). These were all returned to young adult levels by 4 wk postcastration (data not shown). These findings are consistent with the overall reactivation of the thymus. By 2 wk postcastration, expression of MTS24 on thymic epithelium was similar to that seen in young mice (Fig. 1*d*), with scattered medullary patches as opposed to distinct aggregates seen in the aged thymus.

Castration fully normalizes thymocyte differentiation, proliferation, and levels of apoptosis

The aged thymus had <5% cellularity of the young adult ($p \leq 0.01$ at 1 year and $p \leq 0.001$ at 2 years (Fig. 2*a*)). Furthermore, while the proportion of proliferating thymocytes remained constant at ~15–20% of total thymus cellularity at 2 years of age (Fig. 2*b*), their number was markedly reduced ($p \leq 0.001$) (Fig. 2*c*). The rejuvenation of thymopoiesis occurred rapidly following surgical castration of aged (≥2 years) mice such that by 2 wk, thymus cellularity was restored to young adult (2 mo) levels (Fig. 2*a*).

In young mice, proliferation of thymocytes was abundant (Fig. 2*c*) and predominated within the cortical areas (Fig. 2*d*). Thymocyte proliferation was not only greatly reduced numerically in aged mice (Fig. 2*c*), but the areas of proliferation were harder to discern due to the disruption of the microenvironment (Fig. 2*d*). By 2 wk postcastration, thymocyte proliferation was comparable to young mice numerically (Fig. 2*c*) and again localized mainly to the cortical regions (Fig. 2*d*), which is consistent with reorganization of the epithelium. Although the overall proportion of $BrdU^+$ thymocytes remained constant with age and postcastration (Fig. 2*b*), a significant reduction was observed within distinct subsets with age; predominantly within the most immature TN ($\alpha\beta TCR^-CD4^-CD8^-$) and the $CD4^-CD8^+$ and $CD4^+CD8^-$ subsets (both $\alpha\beta TCR^+$ and $\alpha\beta TCR^{low}$) (Fig. 2*e*; $p \leq 0.05$ for TN and $\alpha\beta TCR^{low}CD4^+$ or $CD8^+$ and $p \leq 0.001$ for $\alpha\beta TCR^+CD4^-CD8^+$). These were all significantly increased proportionally as early as 1 wk postcastration ($p \leq 0.05$) and returned to young adult levels by 2 wk postcastration (Fig. 2*e*).

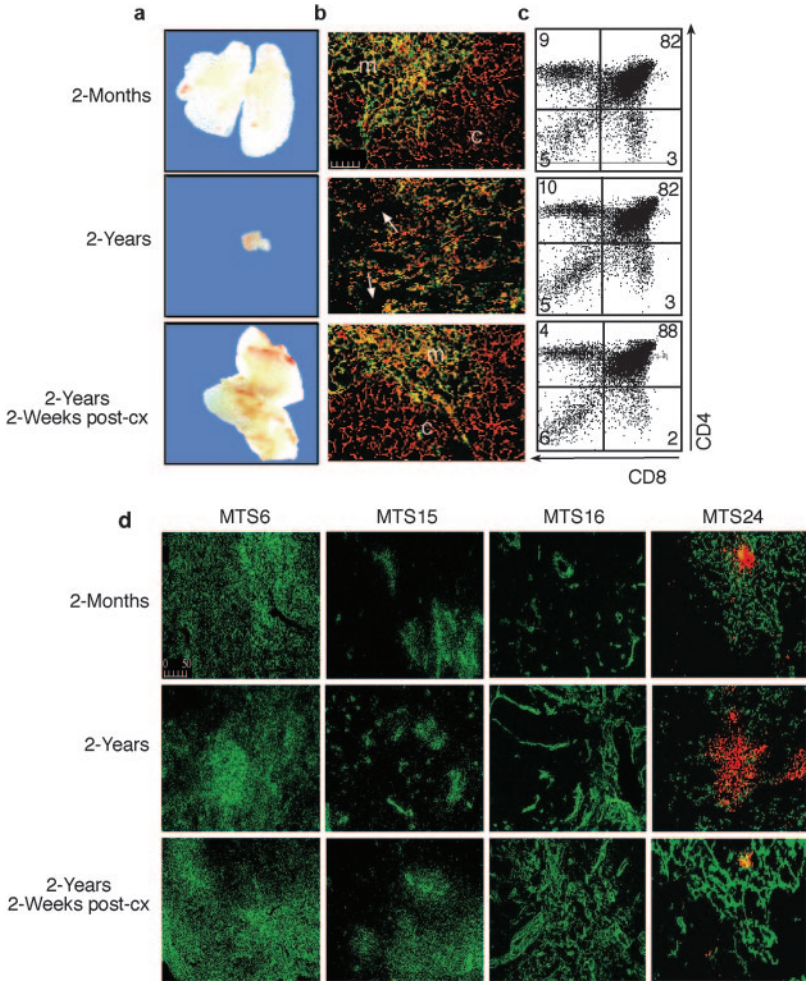

FIGURE 1. All major stromal cell subsets are fully restored postcastration (post-cx). *a*, Gross morphology of the thymus demonstrating the extent of thymus atrophy with age and regeneration by 2 wk post-cx. Images were taken at the same magnification. *b*, Immunofluorescence staining of frozen thymus sections showing anticytokeratin (pan-epithelium; red) and MTS10 (medulla; green/yellow). In the 2-mo thymus, there is a distinct cortex and medulla and well-defined corticomedulla junction (CMJ). With age, there is disruption of the epithelium and an indistinct CMJ. By 2 wk of post-cx, the medulla and cortical areas are indistinguishable from the young adult (2 mo) thymus. Scale = 50 μm. *c*, Representative FACS profiles of CD4/CD8 staining in the thymus. Proportions are given in each quadrant for double-negative, double-positive, CD4, and CD8 cells. There was no difference in the proportion of the major thymocyte subsets with age or post-cx. *d*, Immunofluorescence staining of frozen thymus sections showing MTS6 (detecting MHCII), MTS15 (detecting fibroblasts associated with the vasculature), MTS16 (detecting ECM), and MTS24 (detecting primordial epithelium). The aged thymus shows a reduction in MTS6 expression and an increase in MTS15, MTS16, and MTS24 expression. At 2 wk of post-cx, MTS6, MTS15, and MTS16 were all enhanced in expression while MTS24 expression was comparable to the young adult (2 mo) thymus.

Together with the defects in thymocyte proliferation observed with age, analysis of apoptosis (assessed by Annexin V staining) demonstrated an increase with age (Fig. 2*f*), particularly within the immature, $\alpha\beta TCR^{-/low}$ subsets ($p \leq 0.05$ for double positive; data not shown). The proportion of Annexin V^+ cells returned to young adult levels postcastration (Fig. 2*f*).

Castration rapidly restores proliferation and differentiation within the earliest TN thymocyte subsets

Subdivision of TN cells in aged mice by expression of CD44 and CD25 (Fig. 3*a*) revealed a proportional accumulation of TN1 ($CD44^+CD25^-$) cells ($p \leq 0.001$; Fig. 3, *a* and *b*). Consequently, while the cellularity of all TN subsets was significantly reduced with age ($p \leq 0.001$ for TN2–TN4), this was not as evident within the TN1 subset ($p \leq 0.05$; Fig. 3*c*). The proportion and number of all TN subsets was restored to young adult levels by 1 wk postcastration (Fig. 3, *b* and *c*). Interestingly, a significant reduction in the proportion of c-*kit*$^+$ cells within both the TN1 ($CD44^+CD25^-$; data not shown) and TN2 ($CD44^+CD25^+$) subsets was seen with age ($p \leq 0.01$; Fig. 3, *d* and *e*). This observed reduction in c-*kit* expression has implications for thymocyte development with age because the interaction between c-*kit* and stem cell factor produced by thymic epithelial cells is required for the proliferation and maintenance of TN cells (29). Analysis of TN thymocyte proliferation also revealed a significant decrease in $BrdU^+$ cells within the TN1 subset with age ($p \leq 0.001$; Fig. 3*f*). All of these age-related alterations in the TN subsets were returned to young adult levels by 1 wk postcastration (Fig. 3, *b*, *c*, and *f*), indicating a rapid effect of sex steroid blockade on the earliest stages of thymopoiesis. Importantly, c-*kit* expression was up-regulated on the TN1 and TN2 subsets following castration (Fig. 3, *a* and *d*), coinciding with a significant increase in proliferation of this population ($p \leq 0.05$; Fig. 3*f*).

Molecular analysis of castration-induced thymic reactivation

A key question in this study was the identity of the molecular changes underlying the reversal of thymic atrophy. From the literature, IL-7, TGF-β, and Fgf7 would be likely candidates (30–32). $CD45^-$ thymic stromal cells (incorporating epithelial cells, fibroblasts, and endothelial cells) and whole thymocytes were purified from sham-castrated or castrated mice (9 mo old). Whole stroma was deliberately used due to the production of certain factors by nonepithelium, e.g., Fgf7 by thymic fibroblasts. RT-PCR analysis was performed on equilibrated stromal cell cDNA templates using primers for IL-7, Fgf7, and TGF-β1 and on equilibrated thymocyte cDNA for IL-7R, FgfR2IIIb, and TGF-βRII primers (data not shown). Semiquantitative RT-PCR (Fig. 4*a*) and real-time PCR (Fig. 4*b*) analyses were repeated on at least two separate occasions using different templates (each template consisted of pooled thymii from 10 mice). No consistent change was observed over all time points in any of the genes analyzed (both stroma (Fig. 4) and thymocytes (data not shown)), although inconsistent fluctuations in IL-7 and TGF-β were observed at day 2 postcastration (Fig. 4*b*). This conclusion was also consistent with

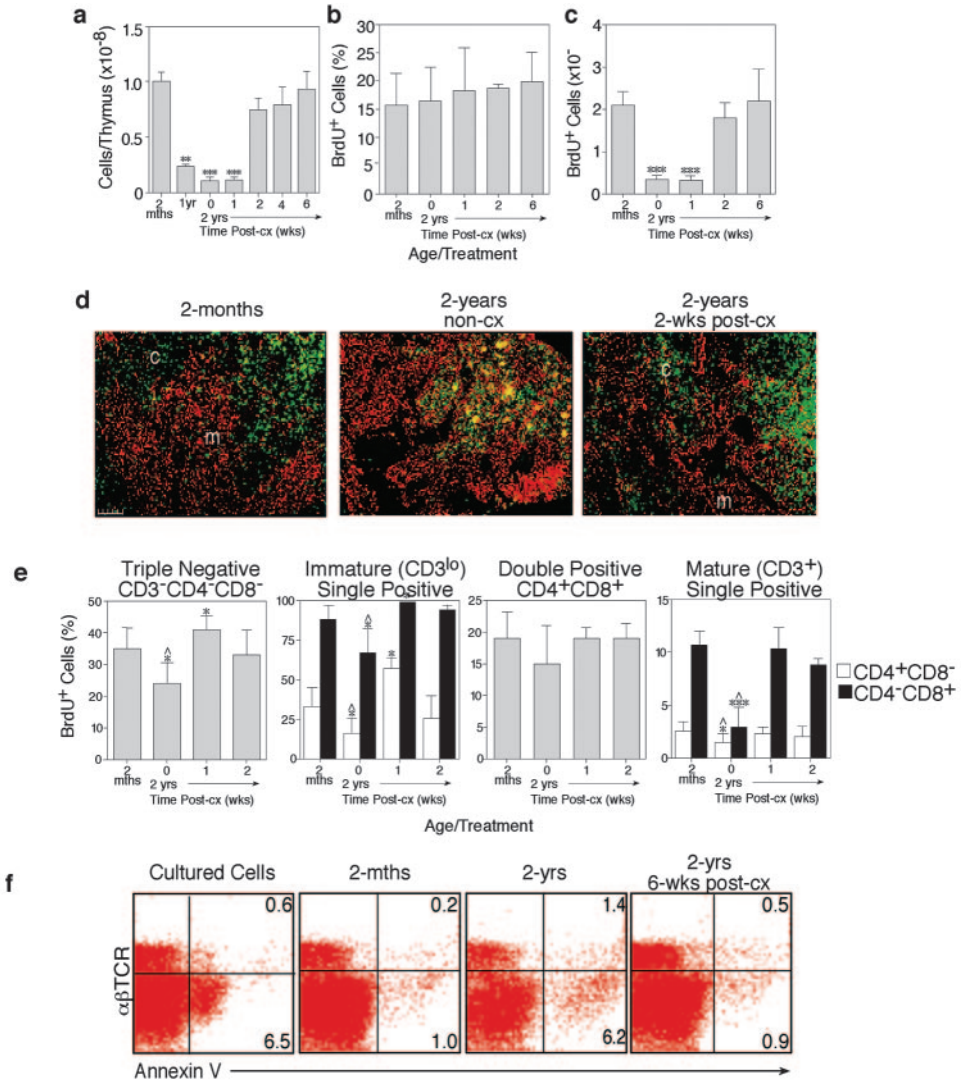

FIGURE 2. Castration increases proliferation and reduces apoptosis, thus fully restoring thymus cellularity. *a*, Aged mice showed a significant reduction in thymus cellularity. By 2 wk postcastration (post-cx), thymocyte numbers were restored to young adult (2 mo) levels. *b*, No change in the percentage of $BrdU^+$ (proliferating) cells was seen with age or post-cx, remaining constant at ~15–20% of total thymocytes. *c*, However, the number of proliferating cells reflected the atrophy of the thymus with age; by 2 wk post-cx, these were similar to the young adult (2 mo) thymus. Results are expressed as mean ± 1SD of 8–12 mice/group. **, $p \leq 0.01$; ***, $p \leq 0.001$ compared with young adult (2 mo) and 2–6 wk post-cx mice. *d*, Immunofluorescence staining of frozen thymus sections showing anticytokeratin (pan-epithelium; red and anti-BrdU (proliferating cells; green)). In the 2-mo thymus, proliferating cells are predominant in the cortex (c), with low levels of $BrdU^+$ cells evident in the medulla (m). With age, the level of proliferation is reduced and is indistinguishable between medulla and cortex. By 2 wk post-cx, intense proliferation is seen within the cortex, which is consistent with the increase in proliferating immature cells as seen by FACS. Scale = 50 μm. *e*, The proportion of $BrdU^+$ cells within the TN and CD8 subsets were significantly decreased with age while a significant increase in the proliferation of $CD3^-CD4^-CD8^+$ immature single-positive (CD8ISP) and mature $CD3^+CD4^-CD8^+$ single-positive cells was seen at 1 wk post-cx. Each bar represents the mean ± 1 SD of four to eight mice. *, $p \leq 0.05$; ***, $p \leq 0.001$ compared with 2-mo-old mice. ^, $p \leq 0.01$ compared with post-cx mice. *f*, Representative FACS profiles of Annexin V vs $\alpha\beta$TCR for detection of apoptotic cells. The aged thymus showed an increase in proportion of apoptotic cells, occurring mainly within the immature ($\alpha\beta TCR^{-/low}$) subsets. This was normalized post-cx. Cultured thymocytes (O/N at 37°C) were used as a positive control.

results found from Affymetrix gene chip analyses of thymic stromal cells postcastration prepared at the same time points (data not shown).

Castration enhances LSK numbers and thymic recovery following BMT

Although sex steroid action on thymic epithelium is required for the induction of thymic atrophy (17), HSC from aged animals are both quantitatively (13) and qualitatively (14) different from those in younger animals. Sex steroids have also been shown to be directly inhibitory on the BM stroma causing a reduction in IL-7 and subsequent B cell production (33–36). The effects on the TN1 subset with age and the rapid rejuvenation of this subset following castration that we observed, prompted us to assess the contribution of HSC to thymic regeneration in a congenic mouse model of BMT. In mice (3–4 mo old) surgically castrated 3 days before reconstitution, there was a significant increase in numbers of LSK (Lin^-c-kit^+sca-1^+, Fig. 5*a*) in the BM at 2 wk post-BMT compared with sham-castrated mice ($p \leq 0.05$; Fig. 5*b*). In addition, total thymus cellularity was significantly increased in castrated mice at both 2 and 4 wk post-BMT ($p \leq 0.05$ and $p \leq 0.01$, respectively) compared with sham-castrated mice (Fig. 5, *c* and *d*). Although residual thymopoiesis was still occurring in the sham-castrated mice (because they were still relatively young), this was

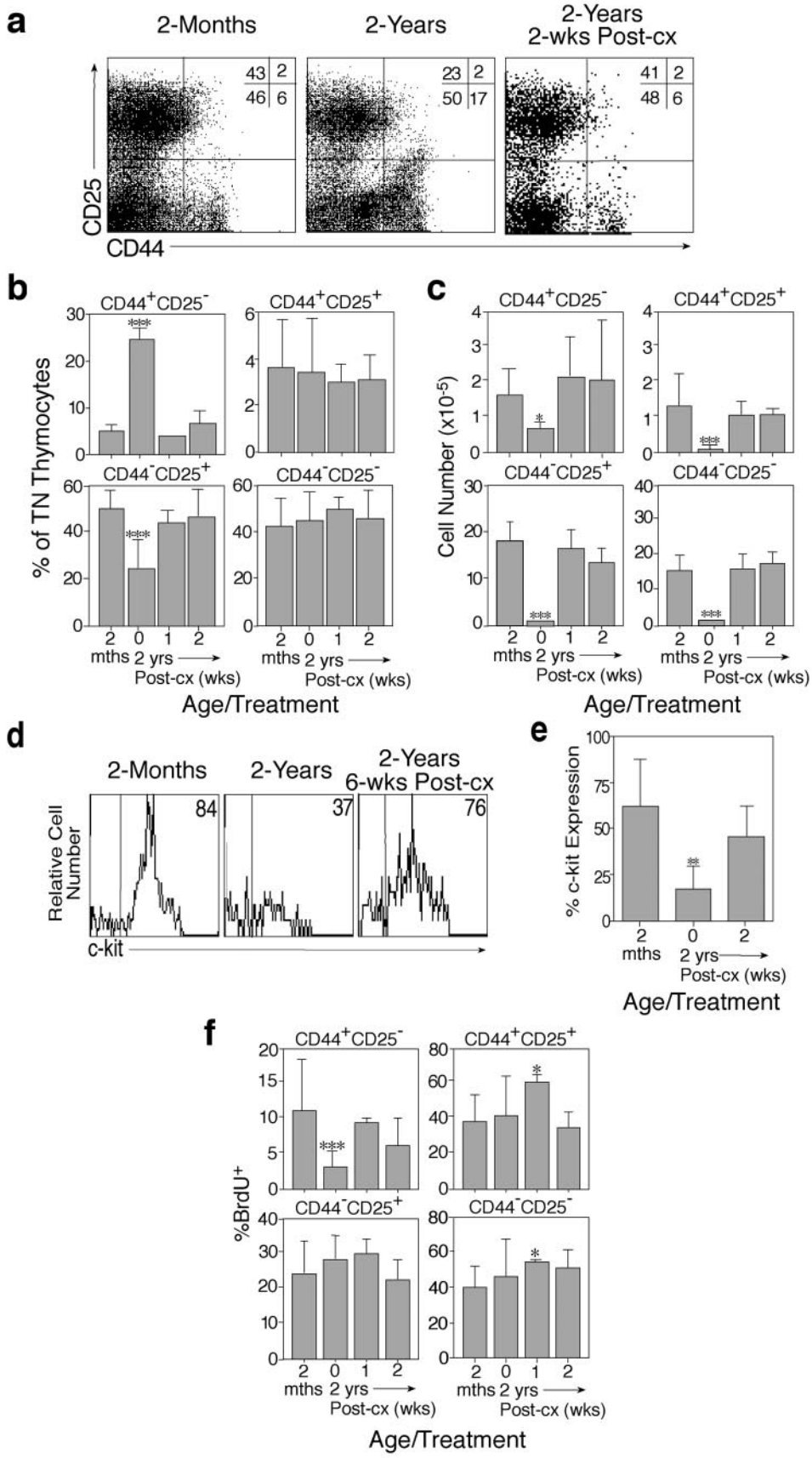

FIGURE 3. Castration rapidly restores defects within the TN thymocyte subpopulations seen with age. *a*, Representative FACS profiles of TN subsets based on the expression of CD44 and CD25. Note the accumulation of the TN1 ($CD44^+CD25^-$) subset with age and their reduction postcastration (post-cx). *b*, Proportion of TN subsets. A significant increase in the proportion of TN1 cells and decrease in proportion of TN3 ($CD44^-CD25^+$) cells was seen with age. These were restored by 1 wk post-cx. Each bar represents the mean ± 1 SD of four to eight mice. ***, $p \leq 0.001$ compared with young (2 mo) and post-cx mice. *c*, Cellularity of TN subsets. A significant decrease in all TN subsets was seen with age and restored by 1 wk post-cx. Each bar represents the mean ± 1 SD of four to eight mice. *, $p \leq 0.05$; ***, $p \leq 0.001$ compared with young (2 mo) and post-cx mice. *d*, Representative FACS histograms showing expression of c-*kit* on TN2 ($CD44^+CD25^+$) cells. *e*, c-*kit* expression was significantly reduced with age and restored post-cx. Each bar represents the mean ± 1 SD of four to eight mice. **, $p \leq 0.01$ compared with 2-mo and postcastrate mice. *f*, The proportion of $BrdU^+$ cells within the TN1 subset was significantly reduced with age and restored by 1 wk post-cx. A significant increase in proportion of $BrdU^+$ cells within the TN2 and TN4 subsets was seen at 1 wk post-cx. Each bar represents the mean ± 1 SD of four to eight mice. *, $p \leq 0.05$ compared with young, aged, and 2-wk post-cx mice; ***, $p \leq 0.001$ compared with young (2 mo) and post-cx mice.

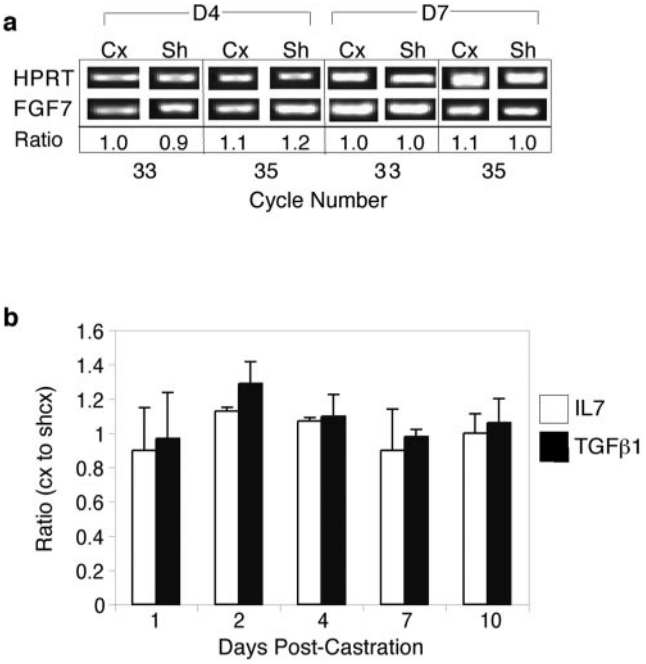

FIGURE 4. Molecular analysis of castration-induced thymic reactivation. *a*, Representative semiquantitative RT-PCR analysis of three separate experiments showing Fgf7 expression in thymic stromal cells from castrated (Cx) and sham-castrated (ShCx) animals at days 4 and 7 postcastration. No consistent difference was observed between Sh and Cx mice at any time point for any factor analyzed. Ratio = equilibration for HPRT expression. *b*, Quantitative real-time PCR analysis of relative IL-7 and TGF-β1 expression at days 1, 2, 4, 7, and 10 postcastration compared with ShCx mice. Results were calculated as the average cycle time of housekeeping gene/average cycle time of test gene and then expressed as a ratio of Cx to ShCx) mice. No change in expression of gene between Cx and Sh is represented by a value of 1. Results are expressed as the mean $\pm$ 1 SD of two separate experiments, 10 mice/group.

significantly reduced compared with the castrated mice. At 2 wk postreconstitution, the majority of LSK were host derived, and this was reflected within the thymus: the majority of thymocytes were also host derived (Fig. 5*d*) in both sham and castrated animals. By 4 wk postreconstitution, at least 99% of LSK were donor derived (data not shown), and this was also reflected in the thymus with the majority of thymocytes being donor derived (Fig. 5*d*). This increase in thymocyte numbers at 4 wk following BMT was also observed when mice were chemically castrated using a LHRH-A 2 wk before reconstitution with allogeneic BM ($p \leq 0.05$; Fig. 5*e*). Consistent with the aging model, thymic structure and proportions of thymocyte subsets following BMT and castration were identical to that of young mice (data not shown). Importantly, intrathymic analysis demonstrated a significant increase in donor-derived DC at 4 wk postreconstitution in castrated mice compared with sham-castrated mice ($p \leq 0.05$; Fig. 5*f*) concentrated at the corticomedullary junction as is normal for host DC (Fig. 5*g*).

Increased thymopoiesis results in increased thymic export and phenotypic restoration of the peripheral T cell pool

To determine whether castration-induced thymic regeneration resulted in changes to thymic export, we used intrathymic FITC injection and assessed the number of $FITC^+$ cells in the periphery within a 24-h period. Previous work has shown that young mice export between 1 and 2×10^6 cells/day, and this is equivalent to 0.5–2% of total thymic cellularity (1, 8, 37), although this rate has been shown to decrease with age (8). Directly aligned with the loss of total thymic cellularity, thymocytes were still being exported but at a much reduced level of $\sim 1 \times 10^5$ thymocytes/day at 15 mo of age (Fig. 6*a*). Despite the major disruption to the thymic microarchitecture in the aged mice, the rate of emigration was still within the normal range (Fig. 6*b*). Following castration-induced activation of thymopoiesis, the number of RTE had significantly increased after only 2 wk ($p \leq 0.01$) and had returned to young levels by 4 wk postcastration (Fig. 6*a*). This increase was also significantly different to that seen at 2 wk postcastration ($p \leq 0.05$), presumably reflecting the differentiation of new precursors through the thymus. The rate of RTE production had decreased slightly at 1 wk postcastration but was significantly increased ($p \leq 0.01$) at 4 wk postcastration compared with sham-castrated mice (although still within normal ranges) (Fig. 6*b*).

The impact of this increased RTE was seen in the proportions of naive ($CD44^{low}$) $CD4^+$ and $CD8^+$ T cells in the periphery after 6 wk (37 $\pm$ 11% postcastration compared with 19 $\pm$ 10% precastration of $CD4^+$ T cells ($p \leq 0.05$) and 52 $\pm$ 9% postcastration compared with 28 $\pm$ 10% precastration of $CD8^+$ T cells ($p \leq 0.01$)) (Fig. 6*c*). This was associated with a corresponding decrease in the proportion (and number; data not shown) of memory ($CD44^{high}$) T cells compared with noncastrated aged mice (Fig. 6*c*). Despite the homeostatic maintenance of total T cell numbers in the periphery (data not shown), a significant decrease ($p \leq 0.01$) in the ratio of CD4:CD8 T cells was seen with age in both the spleen and lymph nodes (Fig. 6*d*). In the young adult, the ratio of CD4:CD8 T cells was $\sim$1.5:1 for both the spleen and lymph nodes, decreasing to $\sim$1:1 in aged mice. The changes observed in the CD4:CD8 ratio were due to a reduction in $CD4^+$ T cells in both the spleen and lymph nodes with age and concomitant increase in $CD8^+$ T cell numbers (data not shown). Castration of the aged mice restored the $CD4^+$ and $CD8^+$ T cell numbers in the spleen and lymph nodes by 6 wk (data not shown), reflected by a normalization of the CD4:CD8 T cell ratio to $\sim$2:1 within the periphery (Fig. 6*d*). In addition, preliminary investigation of TCR repertoire using FACS analysis of TCRVβ regions demonstrated a significant expansion of $V\beta8^+$ within total T cells and $V\beta2^+$ within the $CD4^+$ T cell population in the spleen of aged mice (data not shown). The TCRVβ repertoire was normalized with castration.

Castration restores peripheral T cell function in aged mice

Analysis of splenocyte responsiveness to TCR stimulation (anti-CD3 alone or costimulation with anti-CD28), revealed a significant decrease ($p \leq 0.05$) in proliferation measured by [^{3}H]thymidine incorporation in aged mice (Fig. 7*a*), reflecting the inherent defects in T cell activation associated with age (11). Castration increased the responsiveness to TCR stimulation even above that of young adult mice ($p \leq 0.001$ at 5 μg/ml and $p \leq 0.05$ at 3 and 10 μg/ml; Fig. 7*a*). Aged mice also showed reduced levels of proliferation when costimulation with αCD28 was performed, particularly at a dose of 5 μg/ml αCD3 compared with young adult mice ($p \leq 0.05$) (Fig. 7*a*). By 6 wk postcastration, the level of proliferation in response to αCD3/αCD28 at doses of 1, 3, 5, and 10 μg/ml αCD3 were significantly increased above aged control mice ($p \leq 0.001$, $p \leq 0.001$, $p \leq 0.01$, and $p \leq 0.05$, respectively) (Fig. 7*a*). Castrated mice also showed increased responsiveness above that of young adult levels at a concentration of both 1 and 3 μg/ml αCD3 ($p \leq 0.05$) (Fig. 7*a*).

To further determine the functional consequences of thymus regeneration, we examined the regional (popliteal) lymph node response to human HSV-1 infection (Fig. 7, *b–d*) (38). Although no

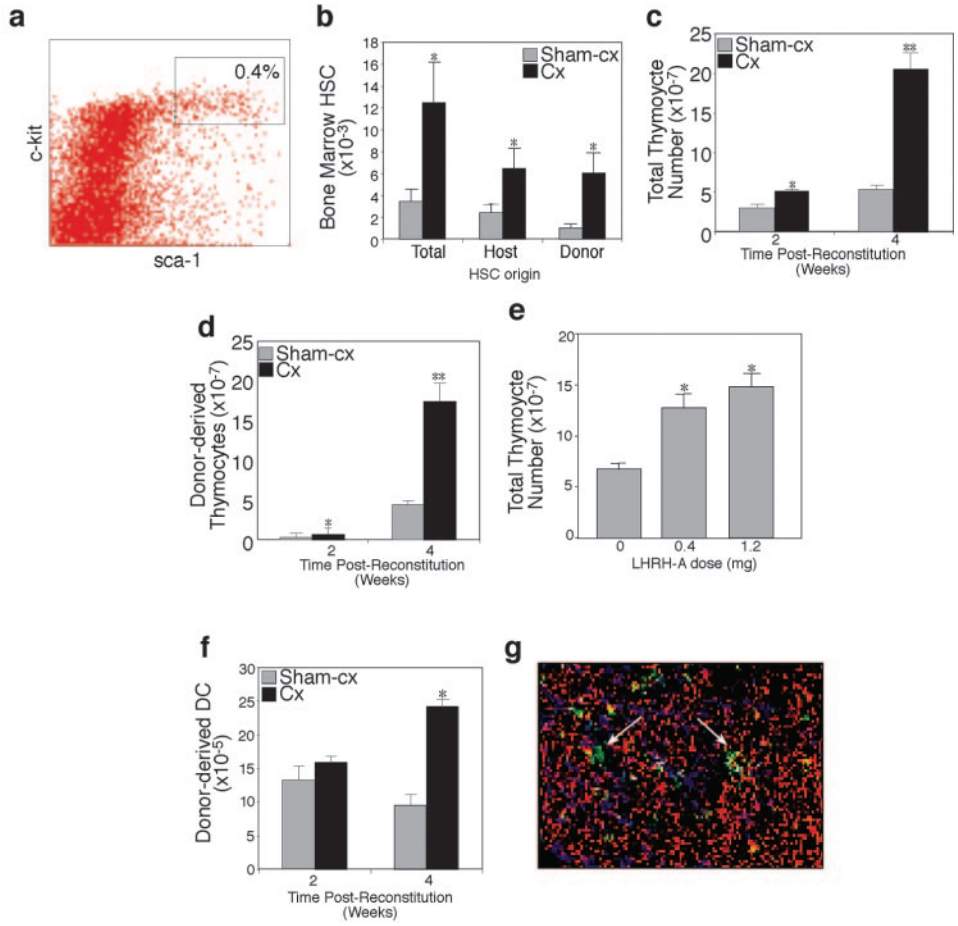

FIGURE 5. Castration enhances stem cell numbers and thymus regeneration following BMT. *a*, Representative FACS dot plots illustrating the detection of LSK. BM cells were gated on Lin^- and analyzed for expression of c-*kit* and sca-1. LSK are defined as Lin^-c-*kit*$^+$sca-1^+. This plot illustrates the proportion seen in castrated (Cx) mice (0.4%) approximately four times higher than young adult unmanipulated mice. (b) Young adult (3–4 mo) mice, surgically Cx before BMT, showed a significantly higher number of LSK compared with sham-Cx mice 2 wk after reconstitution. *c*, Cx mice also showed significantly increased thymus cellularity at both 2 and 4 wk posttransplant compared with sham-Cx mice. (d) In addition, the Cx mice had significantly higher numbers of donor-derived ($Ly5.1^+$) cells/thymus compared with sham-Cx mice. *e*, Chemically Cx (LHRH-A treated) mice showed a significant increase in thymus cellularity at 4-wk (and 6-wk; data not shown) postallogeneic BM reconstitution compared with sham-Cx mice. *f*, The donor-derived cells developed into intrathymic DC with Cx mice showing substantial increases in DC following BMT. *g*, Frozen thymus sections were stained for CD45 (red), CD11c (green), and pan-keratin (blue). The majority of donor-derived DC ($CD45.1^+CD11c^+$) were present at the corticomedullary junction (arrows). Results are expressed as mean ± 1 SD of four to eight mice per group. *, $p \leq 0.05$; **, $p \leq 0.01$ compared with sham-Cx mice.

overt changes in the proportion of the major HSV-specific responding population of $CD25^+CD8^+$ (activated) cells were seen with 18-mo-old compared with 2-mo-old mice (Fig. 7*b*), there was a significant ($p \leq 0.01$) decrease in activated cell number per lymph node in these mice (Fig. 7*c*). Interestingly, a significant reduction in the CD4:CD8 T cell ratio was observed in the resting but not blast T cell populations (data not shown). By 6 wk postcastration, the proportion of responding cells had not changed (Fig. 7*b*), but the total number of activated $CD25^+CD8^+$ cells had increased to young adult levels (Fig. 7c) and a restoration of the CD4:CD8 ratio was observed (data not shown). Furthermore, castration restored the CTL responsiveness to HSV-infected target cells, which was greatly reduced in the aged mice ($p \leq 0.01$) (Fig. 7*d*).

LHRH-agonists enhance thymopoiesis in aged male humans

To assess the clinical potential for restoring thymus function in humans, we analyzed prostate cancer patients (>60 years) who routinely undergo sex steroid ablation therapy based on LHRH-A treatment. They were examined at the time of presentation and after 4 mo of treatment by which time serum testosterone concentration was at castrate levels for all patients (data not shown). A significant increase in total lymphocytes ($p \leq 0.05$), T cells ($p \leq 0.01$) (predominantly $CD4^+$), and NK cells ($p \leq 0.05$) were observed (Fig. 8, *a–c*). More detailed analysis of the T cell compartment revealed a significant increase in the numbers of naive $CD4^+$ T cells ($p \leq 0.05$) and both naive and memory $CD8^+$ T cells ($p \leq 0.05$ for both) following LHRH-A treatment (Fig. 8*d*). There was also a significant increase in the ratio of naive and memory T cells within the $CD4^+$ T cell population (2.3 ± 0.1 before treatment compared with 4.4 ± 1.7 at 4 mo of LHRH-A treatment, $p \leq 0.05$; data not shown).

To determine whether the increase in naive T cells was through peripheral expansion (as seen for example in human cord blood following IL-7 administration (39)) or as a direct result of thymic reactivation, analysis of cellular proliferation (Ki-67 Ag^+) was performed (40). No changes were seen with LHRH-A treatment in proliferation of naive, effector, or memory populations of both $CD4^+$ and $CD8^+$ T cells (remaining at a low 2–4%) (Fig. 8*e*). Direct evidence for an increase in thymic function and T cell export was found following analysis of TREC levels in 10 patients (Fig. 8*f* and

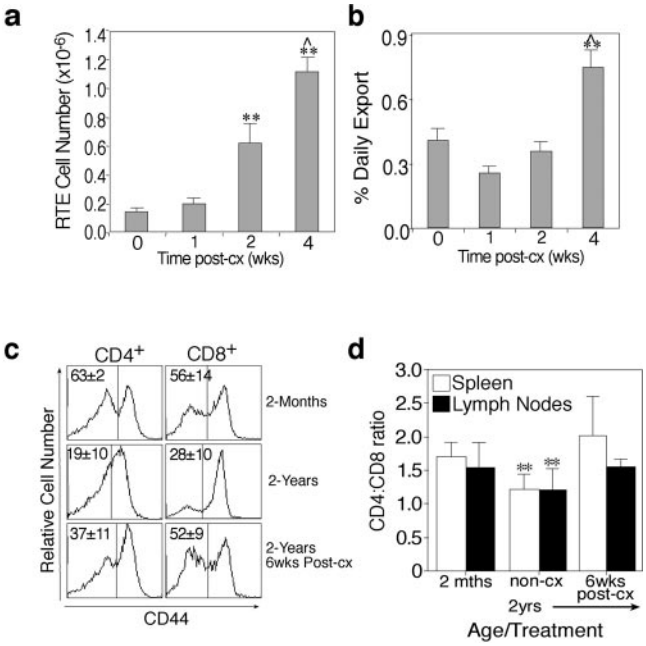

FIGURE 6. Castration results in phenotypic restoration of the peripheral T cell pool. *a*, Following castration of aged mice (13- to 15-mo-old mice were used in *a* and *b*), a significant increase in RTE cell number was observed as early as 2 wk postcastration (post-cx). This had reached young adult levels (data not shown) by 4 wk post-cx. Each bar represents mean ± 1 SD of five to seven mice. For 4 wk post-cx mice, **, $p \leq 0.01$ compared with non-cx and 1 wk post-cx mice. and ^, $p \leq 0.05$ compared with 2-wk post-cx mice. For 2-wk post-cx mice, **, $p \leq 0.01$ compared with aged (non-cx) mice. *b*, In addition, a significant increase in the rate of export (%/thymus/day) was observed by 4 wk post-cx. Note that percent export decreased in the first week post-cx. Each bar represents mean ± 1 SD of five to seven mice. **, $p \leq 0.01$ compared with 2- and 4-wk post-cx mice, and ^, $p \leq 0.05$ non-cx mice. *c*, The increase in export from the postcastrate thymus was reflected by an increase in phenotypically naive ($CD44^{low}$) cells in the spleen. *d*, With age, a significant decrease in the ratio of CD4:CD8 T cells was seen in both the spleen and lymph nodes. By 6 wk post-cx, these values had returned to young adult levels. **, $p \leq 0.01$ compared with young and post-cx mice.

Table I). Within the total TREC population, 6 of 10 patients showed an increase (>25% above initial presentation values) in absolute TREC levels (per milliliter of blood) and proportion (TREC/1 × 10^5 cells; data not shown) by 4 mo of LHRH-A treatment.

Discussion

The present study demonstrates that castration leads to a complete reversal of thymic atrophy in aged male mice, enhanced thymic regeneration following BMT in young male mice, and an increase in thymic-derived T cells in elderly male humans. This occurs via multiple effects on the BM stem cells, the developing thymocytes, and the thymic epithelium.

The impact of androgens and their removal on thymic structure and function has been studied for a number of years (41–43). This study has provided a greater insight into changes in thymocyte and epithelial cell subsets with age and postcastration. The aged (2 years) male mouse thymus showed defects in thymopoiesis throughout multiple stages of development but primarily within the immature thymocyte subsets as seen previously. Castration induced a rapid restoration of thymopoiesis, with significantly enhanced proliferation and reduced apoptosis in the immature subsets evident by 1 wk postcastration. The results found with BrdU incorporation are consistent with findings in young adult animals (42) and demonstrates that the very old thymus, despite the severe atrophy observed, still possesses the ability to respond to appropriate stimuli. Importantly, in very old animals, the impact of castration can be seen at least as long as 1 year after the surgery (unpublished data), whereby, although a gradual reduction in thymocyte cellularity is observed, cellularity within each subset is still significantly increased compared with untreated controls. This is in contrast to findings in young mice, which show only a transient increase in thymic cellularity (25, 41, 42). This most likely reflects the extent of thymic regeneration, particularly of the epithelial component that is required in the aged mouse thymus as distinct to that in the young thymus, which is presumably already highly functional.

Although the location of sex steroid receptors predominates on the epithelial component of the thymus (43), their presence on developing thymocytes have also been shown (44). The major subsets that express these receptors are the $CD4^-CD8^-$ and $CD4^-CD8^+$ subsets—the major subsets showing defects with age in this study. Thus, while it has been clearly shown that receptors on thymic epithelium are required for testosterone-mediated thymic collapse (17), the present study clearly shows that castration effects are manifest at a very early stage on thymocytes. Although this is before epithelial cell division (D. Gray, unpublished observations), it does not exclude the possibility that the T cells are responding to stromal cell-derived stimulatory signals. Interestingly, our results also indicate an effect on the precursor stem cell population in the marrow following castration, suggesting a potential contribution of these cells to thymic regeneration.

An increase in proportion of the TN1 subset was observed with age together with a decrease in proliferation and reduction in expression of c-*kit* (data not shown). It has been shown recently that despite retention of the TN1 proportion with age (16, 45), there is a significant decrease in the early T progenitor (ETP) cells within this population (16), thus leading to numerical reduction of downstream thymocyte subsets. By 1 wk postcastration, the level of proliferation and cellularity of the TN1 population were restored to young adult levels, coinciding with a normalization of c-*kit* expression. Importantly, the rapid restoration of proliferation within the TN1 subset is consistent with data demonstrating the retention of limited functionality within this subset with age. This includes an ability to reconstitute fetal thymic organ culture in vitro (46) and to respond to IL-7 administration in vivo to increase thymopoiesis (47). Current work within our laboratory is looking at the effects of castration on the ETP population to determine their contribution to the regeneration of the involuted thymus.

Preliminary molecular analysis of total thymic stroma following castration (days 1–10) demonstrated no significant alterations in molecules predicted to be important (IL-7, TGF-β, and Fgf7) or their receptors (on thymocytes) (data not shown). Keratinocyte growth factor is not important because FGF7-deficient mice undergo castration induced thymic regeneration (data not shown). It is of obvious importance to assess changes in the molecular microenvironment at distinct time points and within discrete subsets of thymic epithelium/thymocytes. However, in line with our findings, administration of IL-7 to aged mice cannot fully restore the defects in thymopoiesis seen with age (48). This would suggest that more complex events are involved in the recruitment and expansion of thymocyte precursor cells and the thymic microenvironment in general.

The restoration of thymocyte proliferation and differentiation with castration were associated with a full reorganization of the stromal microenvironment such that the castrated thymus was indistinguishable from the young adult thymus in all the cellular and structural parameters examined. Interestingly, immunofluorescence demonstrated a greatly up-regulated expression of MHC class II, ECM, and fibroblasts (associated with the vasculature) at 2 wk postcastration—normalized by 4 wk of postcastration. The

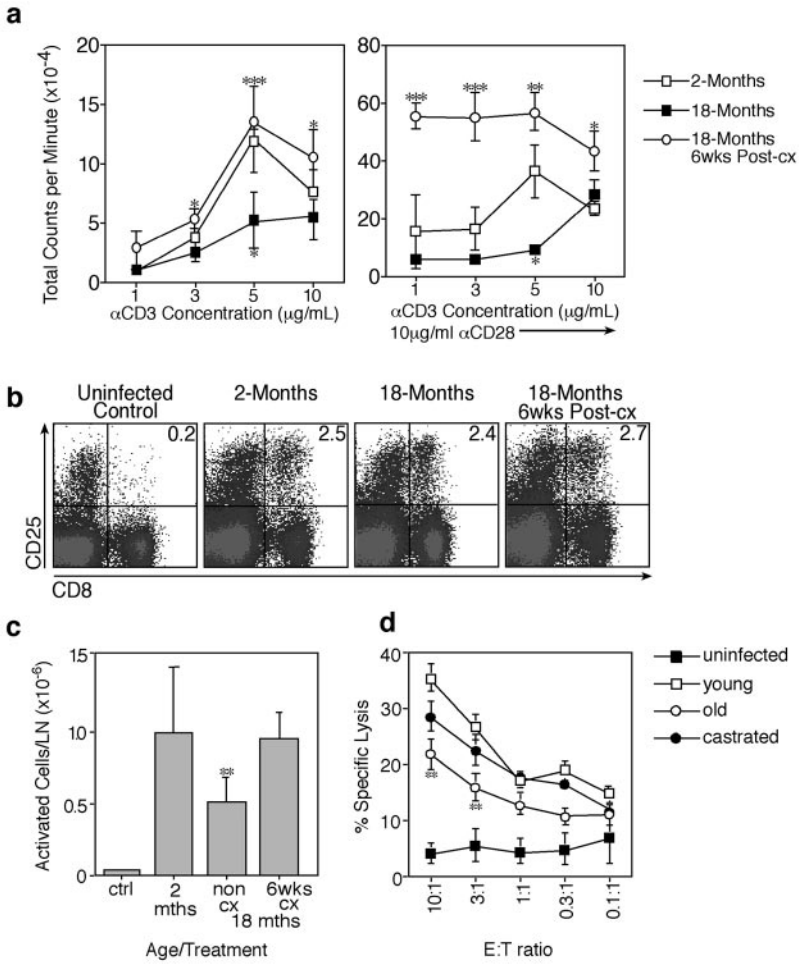

FIGURE 7. Castration restores the peripheral T cell function in aged mice. *a*, The phenotypic changes in the peripheral T cell pool with castration were reflected by a significant increase in [^{3}H]thymidine incorporation following in vitro TCR (anti-CD3) stimulation (*left panel*), particularly with anti-CD28 costimulation (*right panel*). Results are expressed as mean ± 1 SD of triplicate results from four mice per group. *, $p \leq 0.05$ compared with 3-mo-old mice; *, $p \leq 0.05$; **, $p \leq 0.01$; ***, $p \leq 0.001$ compared with 18-mo-old mice. *b*, FACS dot plots illustrating analysis of activated lymph node cells ($CD8^+CD25^+$) following HSV infection. No difference in proportion was observed with age or postcastration (post-cx). *c*, However, a significant decrease ($p \leq 0.01$) in activated ($CD8^+CD25^+$) cell numbers was observed with age, correlating with a significant decrease in total lymph node cellularity (data not shown). Castration of the aged mice restored the immune response to HSV-1, with CTL numbers equivalent to young mice. Results are expressed as mean ± 1 SD of eight to twelve mice. *d*, Aged mice showed a significant reduction in CTL activity at an E:T ratio of both 10:1 and 3:1. Castrated mice demonstrated a comparable response to HSV-1 as the young adult mice. Results are expressed as mean of eight mice in triplicate ± 1 SD. **, $p \leq 0.01$ compared with control and Cx mice.

results obtained by immunofluorescence are supported by flow cytometric analysis demonstrating a significant proportional decrease in MHC class II^{high} epithelial cells with age (12 mo), which returned to normal young levels within 2 wk postcastration (D. H. D. Gray et al., manuscript in preparation). Another striking feature of the aged thymus was the cortical disruption and concurrent aggregation of putative thymic stem cells ($MTS24^+$ epithelium), apparently in higher proportions than in the young thymus. Interestingly, while a numerical decrease was seen in all epithelial subsets with age and all showed subsequent expansion postcastration, the highest increase was within the medullary epithelium. The $MTS24^+$ cells remained relatively similar as a proportion of the total epithelium (D. H. D. Gray et al., manuscript in preparation). The developmental relationships between the cortical, medullary, and $MTS24^+$ cells in this epithelial recovery are currently unknown, but castration-induced thymic regeneration does not selectively stimulate expansion of the $MTS\text{-}24^+$ epithelial subset. Although it remains to be shown whether there are any functional changes induced, it should be noted that the adult $MTS\text{-}24^+$ epithelium does not seem to possess the same capacity for survival as their embryonic counterparts (28). Current work is involved in determining the rate of turnover of the separate epithelial subsets and their lineage relationships.

The increase in thymus cellularity postcastration of aged mice resulted in significantly increased export of RTE to the periphery. This in turn induced phenotypic changes within the peripheral T cell pool, including a normalization of the low CD4:CD8 T cell ratio seen with age, an increase in the proportion of naive T cells, and a resultant decrease in memory cells. The phenotypic changes in the peripheral T cell pool were associated with pronounced changes in T cell function. Aged mice showed a decreased capacity for proliferation following TCR stimulation. This is likely to be predominantly due to inherent defects in intracellular signaling pathways (11) with age but may also relate to levels of CD28 expression (49), resulting in a loss in the costimulatory capacity of aged T cells. Castration restored the T cell response to TCR triggering (and costimulation) in aged mice. Importantly, castration also enhanced the immune response of aged mice to viral infection. The development of specific CTL immune response to HSV-1 requires interaction between $CD4^+$ T cells and APC (50, 51) and the need for massive infiltration of naive $CD8^+$ T cells to the site of infection (38, 52). Although aged mice were consistently able to produce similar proportions of activated $CD8^+$ T cells as young adult mice following infection, a decrease in total draining lymph node cellularity and therefore activated cell numbers was seen. As a consequence, aged mice showed a decreased ability to generate CTL-specific responses compared with both young adult and postcastrate mice. This may be due to the inherent inability of T cells from aged mice to secrete IL-2 upon stimulation (11), which is required for generation of an efficient HSV-specific response (52). Castration restored the responsiveness to HSV to levels equivalent to those seen in young mice, possibly relating to a restoration of the CD4:CD8 T cell ratio in the resting lymph node population (data not shown). It would be of interest to assess the function of APC in this model because these have been shown to be defective in aged mice (53), are vital for proper viral responsiveness (50), and are able to be modulated by sex steroids (54).

It is possible that removal of sex steroids is having direct functional consequences on the peripheral T cells. The presence of

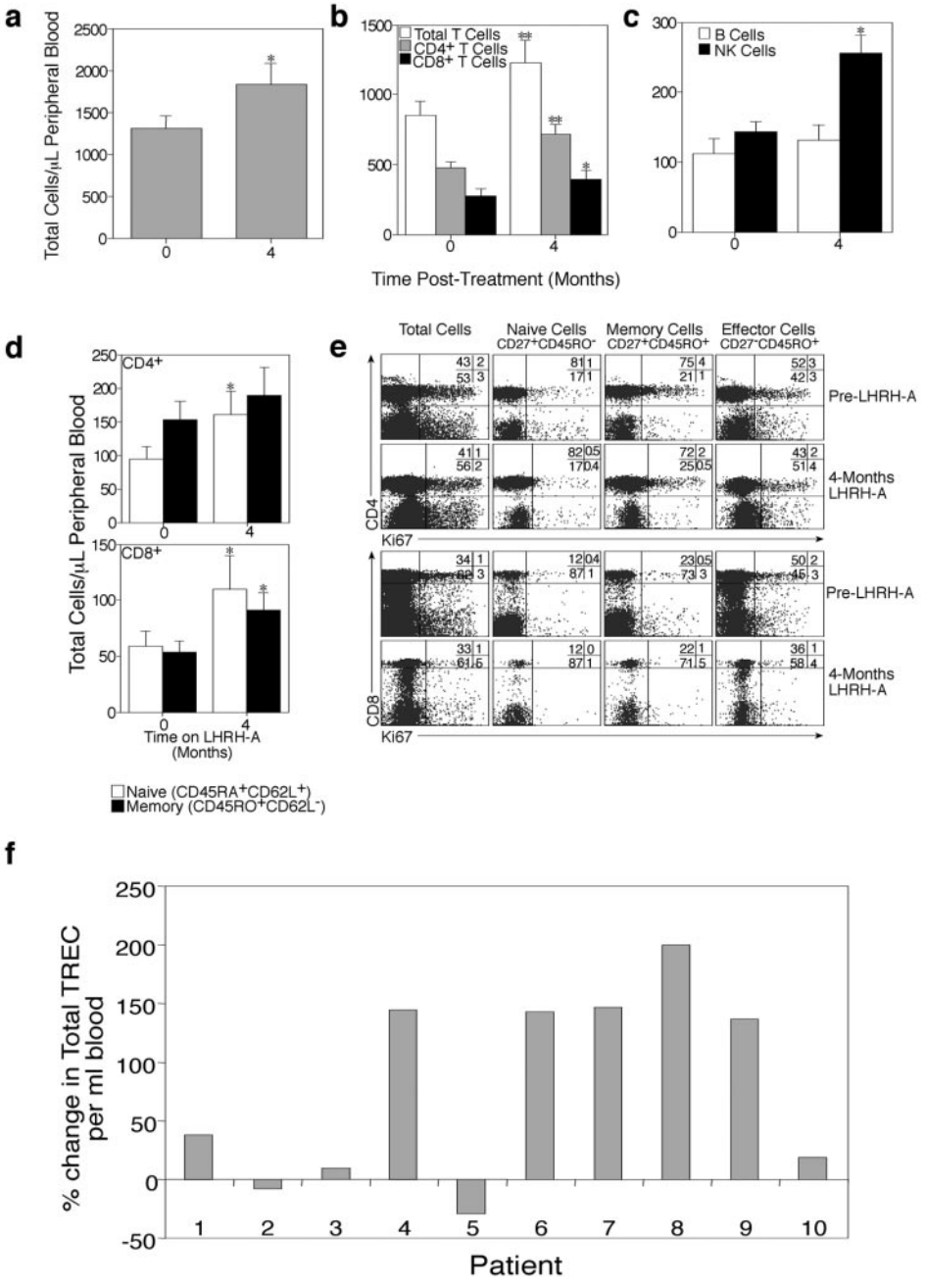

FIGURE 8. Chemical castration in humans enhances thymus function. *a*, Total lymphocyte number per microliter peripheral blood was significantly increased following LHRH-A treatment. *b*, This was reflected by a significant increase in total T cells and $CD4^+$ and $CD8^+$ T cells. *c*, Although a significant increase in NK cell numbers was also observed, B cells were not altered with treatment. *d*, A significant increase in naive ($CD62L^+CD45RA^+CD45RO^-$) $CD4^+$ and both naive and memory ($CD62L^-CD45RA^-CD45RO^+$) $CD8^+$ T cells was observed with the agonist treatment. Each bar represents the mean ± 1 SD of 16 patients. *, $p \leq 0.05$; **, $p \leq 0.01$ compared with pretreatment values. *e*, Analysis of cellular proliferation was performed using Ki-67 Ag detection. In all patients, levels of proliferation within naive, effector, and memory cell subsets for both $CD4^+$ and $CD8^+$ T cells was not altered with LHRH-A treatment. *f*, Analysis of TREC levels in the peripheral blood. At 4 mo post-LHRH-A treatment, 8 of 10 patients showed increases in total $TREC^+$ cells/milliliter blood compared with pretreatment. In 6 of 10 patients, these were deemed substantial (>25% increase). One patient showed a substantial decrease.

testosterone receptors on peripheral T cells (55) indicates that removal of the suppressive effects of testosterone could directly enhance the proliferation of these cells. However, while loss of sex steroids may directly contribute to the rejuvenation of peripheral T cell responses, the observed increase in $FITC^+$ RTE, the proportion of naive T cells and diversity of the TCR repertoire can only be achieved through thymic output. Therefore, castration not only restored thymus integrity in aged mice but also rectified phenotypic and functional T cell specific defects in the periphery.

A major finding from this study was the enhanced regeneration of thymus cellularity following BMT in young mice with surgical or chemical castration. It is still unclear precisely what role changes in progenitor cells play in the aging-induced atrophy and its reversal by castration. The latter may involve normalization of the intrathymic progenitors or an increased number of marrow-derived progenitors, which then differentiate normally, or both these alternatives. In this study, sex steroid ablation resulted in a significant increase in LSK content within the BM and enhanced numbers of donor-derived LSK, which developed into DC and T cells in numbers and proportion similar to the normal young thymus. This occurred in two waves: the first 2 wk showed development of radio-resistant host-precursor cells, and following this, development of donor-LSK (the marrow was 100% donor-derived at this stage) occurred. Additional studies, including in vivo bioluminescence imaging, may help to determine whether castration actively promotes the thymic uptake of stem cells or induces them to undergo intrathymic proliferation and differentiation at a faster rate. Although we have shown that castration is essential for restoration of the aged thymic microenvironment, it is highly likely that this is at least partly due to an increase in HSC number and/or function. This is currently under investigation in our laboratory with secondary transfer of the donor stem cells being performed.

The importance of increasing HSC numbers in the periphery is exemplified in a study by Douek et al. (23), whereby enriching for

Table I. *TREC levels following LHRH-A treatment in humans*[a]

	$CD4^+$ T Cells			$CD8^+$ T Cells			Total TRECs		
Patient	Pre	Post	% Change	Pre	Post	% Change	Pre	Post	% Change
1	710	158	↓ 78	U/D	824	N/A	710	982	↑ 38
2	4142	2645	↓ 36	680	1771	↑ 160	4822	4416	↓ 8
3	1265	1031	↓ 18	536	950	↑ 77	1801	1981	↑ 10
4	502	3242	↑ 546	1206	950	↓ 21	1709	4192	↑ 145
5	1862	1191	↓ 36	584	541	↓ 7	2446	1732	↓ 29
6	571	2378	↑ 316	407	U/D	N/A	978	2378	↑ 143
7	176	705	↑ 300	187	191	↑ 2	363	897	↑ 147
8	2716	5349	↑ 97	1293	6688	↑ 417	4008	12037	↑ 200
9	3289	8561	↑ 160	1474	2715	↑ 84	4763	11276	↑ 137
10	2922	3582	↑ 23	389	361	↓ 7	3312	3943	↑ 19

[a] Pre indicates TREC levels before LHRH-A treatment; post indicates TREC levels at 4-mo of treatment with LHRH-A. ↑, increase; ↓, decrease. U/D, undetectable levels for sensitivity of assay (<100 copies)—designated as "0" for the purpose of analysis; N/A, percentage of change could not be determined for sample because of U/D levels at one time point. Results are expressed as TREC levels within the FACS sorted $CD4^+$,$CD8^+$ per milliliter of peripheral blood. Total TREC indicates the total number of TRECs calculated from the sorted populations (sum of $CD4^+$ and $CD8^+$ TRECs).

$CD34^+$ T cells before hemopoietic transplantation in humans resulted in significantly increased levels of TREC compared with recipients of unmanipulated grafts. The observed increase in the intrathymic conversion of LSK to donor-derived DC may also facilitate the establishment of central tolerance for graft acceptance of the same donor type (56). This has been shown experimentally using murine allogeneic transplants, the presence of intrathymic donor DC being closely associated with longer-term kidney graft acceptance (57).

Analysis of patients undergoing LHRH-A as part of their routine treatment for prostate cancer demonstrated the ability of chemical castration to increase thymic-dependent T cell production in aged humans. In all patients, an increase in lymphocyte numbers was observed following LHRH-A treatment (4 mo) confirming previous findings (58–60). However, the present study expanded on these findings by demonstrating that the increase in lymphocyte numbers is predominantly due to an increase in T cells—both $CD4^+$ and $CD8^+$. This may be partly due to direct stimulation of peripheral T cells by LHRH-A (61) or an indirect effect due to loss of sex steroids. However, we were also able to demonstrate a significant increase in specific, naive T cells following treatment with the agonist with analysis of TREC levels in the periphery demonstrating that chemical castration is inducing reactivation of the thymic-dependent T cell pathway in aged humans. Interestingly, a disparate increase in $TREC^+CD4^+$ vs $TREC^+CD8^+$ levels was observed. This indicates that either a greater proportion of $CD4^+$ to $CD8^+$ T cells are migrating to the periphery or that the $CD8^+$ T cells are induced to undergo antigenic proliferation at a faster rate than the $CD4^+$ T cells, thereby diluting out TREC levels. In aged mice postcastration, a significant increase in mature $CD8^+$ thymocyte proliferation was seen compared with $CD4^+$ single-positive cells. Therefore, TREC levels could also be reduced intrathymically before export. Regardless, the levels of TREC in the periphery will never be an overestimate, and because excessive proliferation was not observed in these patients with LHRH-A administration, they are probably a true indication of steady-state levels of T cell emigration in aged humans. LHRH-ARs are present on both peripheral lymphocytes (62) and also within the thymic microenvironment (63). It is interesting to speculate that the mode of action of LHRH-A could, at least in part, be due to a direct, immunomodulatory role of LHRH-A on the immune system. In support of this, aging is associated with a severe reduction in LHRH-A binding sites within the thymus of both female and male rats and this is fully reversed with LHRH-A treatment (63).

One of the most important features of this method of thymic reactivation is that it involves a simple blockade of sex steroid production, effectively returning the thymus to its prepubertal state. Once the sex steroids are removed, the thymus presumably uses its inherent regulatory control mechanisms over cellular proliferation, cytokine levels, and the full complement of the thymic microenvironment to efficiently generate normal T cell production, without requiring the addition of exogenous cytokines. As a consequence, there has been no evidence of pathological conditions developing, particularly autoimmune. Indeed, the enhanced effectiveness of the T cell arm of the immune response through regeneration of the naive T cell repertoire may be an important feature of the control of prostate cancer (64). The treatment via chemical castration is also completely reversible, with normal sex steroid levels returning after the removal of the LHRH-A (65). The incorporation of sex-steroid ablation therapy in combination with autologous or exogenous HSC, which themselves could be manipulated for gene therapy (particularly relevant in the setting of HIV/AIDS (for example)) sets a fundamentally new foundation for the immunotherapy of T cell-based disorders.

Acknowledgments

We thank Assoc. Prof. Frank Carbone for the HSV, Dr. Paul Cameron for cell sorting, Professor Sharon Lewin and Ajantha Solomon for TREC analysis, Jade Barbuto for help with stromal cell isolation, Morag Milton for assistance with the real-time PCR analysis, and Drs. Victor Lee and John Funder for the initial castration studies. We also acknowledge Peter Simpson of Norwood Abbey Ltd. and the invaluable support of the company.

Disclosures

The authors have no financial conflict of interest.

References

1. Berzins, S. P., R. L. Boyd, and J. F. A. P. Miller. 1998. The role of the thymus and recent thymic migrants in the maintenance of the adult peripheral lymphocyte pool. *J. Exp. Med.* 187: 1839–1848.
2. Hirokawa, K., M. Utsuyama, M. Kasai, C. Kurashima, S. Ishijima, and Y. X. Zeng. 1994. Understanding the mechanism of the age-change of thymic function to promote T cell differentiation. *Immunol. Lett.* 40: 269–277.
3. Tosi, P., R. Kraft, P. Luzi, M. Cintorino, G. Fankhause, M. W. Hess, and H. Cottier. 1982. Involution pattern of the human thymus. I. Size of the cortical area as a function of age. *Clin. Exp. Immunol.* 47: 497–504.
4. Windmill, K. F., and V. W. K. Lee. 1998. Effects of castration on the lymphocytes of the thymus, spleen and lymph nodes. *Tissue Cell* 30: 104–111.
5. Greenstein, B. D., F. T. A. Fitzpatrick, M. D. Kendall, and M. J. Wheeler. 1987. Regeneration of the thymus in old male rats treated with a stable analogue of LHRH. *J. Endocr.* 112: 345–350.
6. Greenstein, B. D., F. T. A. Fitzpatrick, I. M. Adcock, M. D. Kendall, and M. J. Wheeler. 1986. Reappearance of the thymus in old rats after orchidectomy: inhibition of regression by testosterone. *J. Endocrinol.* 110: 417–425.
7. Windmill, K. F., B. J. Meade, and V. W. K. Lee. 1993. Effect of prepubertal gonadectomy and sex steroid treatment on the growth and lymphocyte populations of the rat thymus. *Reprod. Fertil. Dev.* 5: 73–81.

8. Scollay, R. G., E. C. Butcher, and I. L. Weissman. 1980. Thymus cell migration: quantitative aspects of cellular traffic from the thymus to the periphery in mice. *Eur. J. Immunol.* 10: 210–218.
9. Nicoletti, C. 1994. Antibody response in aged C57BL/6 mice: T helper cells are responsible for the decline of the primary antibody response to a bacterial antigen in aging. *Immunobiology* 190: 127–137.
10. Bloom, E. T., H. S. Mostowski, and J. A. Horvath. 1994. Does the age-related change in CD44-defined T cell subsets have functional significance for cytotoxic T lymphocyte generation? *Immunol. Lett.* 40: 251–258.
11. Hertogh-Huijbregts, A., C. Vissinga, J. Rozing, and L. Nagelkerken. 1990. Impairment of CD3-dependent and CD3-independent activation pathways in $CD4^+$ and in $CD8^+$ T cells from old CBA/RIJ mice. *Mech. Ageing Dev.* 53: 141–155.
12. Boyd, R. L., C. L. Tucek, D. I. Godfrey, T. J. Wilson, N. J. Davidson, A. G. D. Bean, H. M. Ladyman, M. A. Ritter, and P. Hugo. 1993. The thymic microenvironment. *Immunol. Today* 14: 445–459.
13. Eren, R., A. Globerson, L. Abel, and D. Zharhary. 1990. Quantitative analysis of bone marrow thymic progenitors in young and aged mice. *Cell. Immunol.* 127: 238–246.
14. Sudo, K., H. Ema, Y. Morita, Y., and H. Nakauchi. 2000. Age-associated characteristics of murine hematopoietic stem cells. *J. Exp. Med.* 192: 1273–1280.
15. Fridkis-Hareli, M., L. Abel, and A. Globerson. 1992. Patterns of dual lymphocyte development in co-cultures of foetal thymus and lymphohaemopoietic cells from young and old mice. *Immunology* 77: 185–188.
16. Min, H., E. Montecino-Rodriquez, and K. Dorshkind. 2004. Reduction in the developmental potential of intrathymic T cell progenitors with age. *J. Immunol.* 173: 245–250.
17. Olsen, N. J., G. Olson, S. M. Viselli, X. Gu, and W. J. Kovacs. 2001. Androgen receptors in thymic epithelium modulate thymus size and thymocyte development. *Endocrinology* 142: 1278–1283.
18. Sempowski, G. D., L. P. Hale, J. S. Sundy, J. M. Massey, R. A. Koup, D. C. Douek, D. D. Patel, and B. F. Haynes. 2000. Leukemia inhibitory factor, oncostatin M, IL-6, and stem cell factor mRNA expression in human thymus increases with age and is associated with thymic atrophy. *J. Immunol.* 164: 2180–2187.
19. Douek, D. C., and R. A. Koup. 2000. Evidence for thymic function in the elderly. *Vaccine* 18: 1638–1641.
20. Jamieson, B. D., D. C. Douek, S. Killian, L. E. Hultin, D. D. Scripture-Adams, J. V. Giorgi, D. Marelli, R. A. Koup, and J. A. Zack. 1999. Generation of functional thymocytes in the human adult. *Immunity* 10: 569–575.
21. Douek, D. C., R. D. McFarland, P. H. Keiser, E. A. Gage, J. M. Massey, B. F. Haynes, M. A. Polis, A. T. Haase, M. B. Feinberg, J. L. Sullivan, et al. 1998. Changes in thymic function with age and during the treatment of HIV infection. *Nature* 396: 690–695.
22. Heitger, A., H. Greinix, C. Mannhalter, D. Mayerl, H. Kern, J. Eder, F.-M. Fink, D. Niederwieser, and E.-R. Panzer-Grumayer. 2000. Requirement of residual thymus to restore normal T cell subsets after human allogeneic bone marrow transplantation. *Transplantation* 69: 2366–2373
23. Douek, D. C., R. A. Vescio, M. R. Betts, J. M. Brenchley, B. J. Hill, L. Zhang, J. R. Berenson, R. H. Collins, and R. A. Koup. 2000. Assessment of thymic output in adults after haematopoietic stem-cell transplantation and prediction of T cell reconstitution. *Lancet* 355: 1875–1881.
24. Weinberg, K., B. R. Blazar, J. E. Wagner, E. Agura, B. J. Hill, M. Sorgorzewska, R. A. Koup, M. R. Betts, R. H. Collins, and D. C. Douek. 2001. Factors affecting thymic function after allogeneic hematopoietic stem cell transplantation. *Blood* 97: 1457–1466.
25. Roden, A. C., M. T. Moser, S. D. Tri, M. Mercader, S. M. Kuntz, H. Dong, A. A. Hurwitz, D. J. McKean, E. Celis, B. C. Leibovich, J. P. Allison, and E. D. Kwon. 2004. Augmentation of T cell levels and responses induced by androgen deprivation. *J. Immunol.* 173: 6098.
26. Gray, D. H. D., A. C. Chidgey, and R. L. Boyd. Analysis of thymic stromal cell populations using flow cytometry. 2002. *J. Immunol. Methods* 260: 15–28
27. Zhang, L., S. R. Lewin, M. Markowitz, H.-H. Lin, E. Skulsky, R. Karanicolas, Y. He, X. Jin, S. Tuttleton, M. Vesanen, et al. 1999. Measuring recent thymic emigrants in blood of normal and HIV-1-infected individuals before and after effective therapy. *J. Exp. Med.* 190: 725–732.
28. Gill, J. W., M. A. Malin, G. A. Hollander, and R. L. Boyd. 2002. Generation of a complete thymic microenvironment by $MTS24^+$ thymic epithelial cells. *Nat. Immunol.* 3: 635–642.
29. Godfrey, D. I., J. Kennedy, T. Suda, and A. Zlotnik. 1993. A developmental pathway involving four phenotypically and functionally distinct subsets of $CD3^-CD4^-CD8^-$ triple-negative adult mouse thymocytes defined by CD44 and CD25 expression. *J. Immunol.* 150: 4244–4252.
30. von Freeden-Jeffry, U., N. Solvason, M. Howard, and R. Murray. 1997. The earliest T lineage-committed cells depend on IL-7 for Bcl-2 expression and normal cell cycle progression. *Immunity* 7: 147–154.
31. Takahama, Y., J. J. Letterio, H. Suzuki, A. G. Farr, and A. Singer. 1994. Early progression of thymocytes along the CD4/CD8 developmental pathway is regulated by a subset of thymic epithelial cells expressing transforming growth factor β. *J. Exp. Med.* 179: 1495–1506.
32. Erickson, M., S. Morkowski, S. Lehar, G. Gillard, C. Beers, J. Dooley, J. S. Rubin, A. Rudensky, and A. D. Farr. 2002. Regulation of thymic epithelium by keratinocyte growth factor. *Blood* 100: 3269–3278.
33. Kincade, P. W., K. L. Medina, and G. Smithson. 1994. Sex hormones as negative regulators of lymphopoiesis. *Immunol. Rev.* 137: 119–134.
34. Jonsson, J.-I., and R. A. Phillips. 1993. Interleukin-7 responsiveness of $B220^+$ B cell precursors from bone marrow decreases in aging mice. *Cell. Immunol.* 147: 267–278.
35. Stephan, R. P., C. R. Reilly, and P. L. Witte. 1998. Impaired ability of bone marrow stromal cells to support B-lymphopoiesis with age. *Blood* 91: 75–88.
36. Olsen, N. J., X. Gu, and W. J. Kovacs. 2001. Bone marrow stromal cells mediate androgenic suppression of B lymphocyte development. *J. Clin. Invest.* 108: 1697–1704.
37. Berzins, S. P., E. S. Venanzi, C. Benoist, and D. Mathis. 2003. T cell compartments of prediabetic NOD mice. *Diabetes* 52: 327–334.
38. Cose, S. C., C. M. Jones, M. E. Wallace, W. R. Heath, and F. R. Carbone. 1997. Antigen-specific $CD8^+$ T cell subset distribution in lymph nodes draining the site of herpes simplex virus infection. *Eur. J. Immunol.* 27: 2310–2316.
39. Soares, M. V. D., N. J. Borthwick, M. K. Maini, G. Janossy, M. Salmon, and A. N. Akbar. 1998. IL-7-dependent extrathymic expansion of $CD45RA^+$ T cells enables preservation of a naive repertoire. *J. Immunol.* 161: 5909–5917.
40. Hazenberg, M. D., M. C. Verschuren, D. Hamann, F. Miedema, and J. J. van Dongen. 2001. T cell receptor excision circles as markers for recent thymic emigrants: basic aspects, technical approach, and guidelines for interpretation. *J. Mol. Med.* 79: 631–640.
41. Viselli, S. M., S. Stanziale, K. Shults, W. J. Kovacs, and N. J. Olsen. 1995. Castration alters peripheral immune function in normal male mice. *Immunology* 84: 337–342.
42. Olsen, N. J., S. M. Viselli, K. Shults, G. Stelzer, and W. J. Kovacs. 1994. Induction of immature thymocyte proliferation after castration of normal male mice. *Endocrinology* 134: 107–113.
43. Savino, W., and M. Dardenne. 2000. Neuroendocrine control of thymus physiology. *Endocr. Rev.* 21: 412–443.
44. Viselli, S. M., N. J. Olsen, K. Shults, G. Steizer, and W. J. Kovacs. 1995. Immunochemical and flow cytometric analysis of androgen receptor expression in thymocytes. *Mol. Cell. Endocrinol.* 109: 19–26.
45. Aspinall, R. 1997. Age-associated thymic atrophy in the mouse is due to a deficiency affecting rearrangement of the TCR during intrathymic T cell development. *J. Immunol.* 158: 3037–3045.
46. Aspinall, R., and D. Andrew. 2001. Age-associated thymic atrophy is not associated with a deficiency in the $CD44^+CD25^-CD3^-CD4^-CD8^-$ thymocyte population. *Cell. Immunol.* 212: 150–157.
47. Andrew, D., and R. Aspinall. 2001. IL-7 and not stem cell factor reverses both the increase in apoptosis and the decline in thymopoiesis seen in aged mice. *J. Immunol.* 166: 1524–1530.
48. Sempowski, G. D., M. E. Gooding, H. X. Liao, P. T. Le, and B. F. Haynes. 2002. T cell receptor excision circle assessment of thymopoiesis in aging mice. *Mol. Immunol.* 38: 841–848
49. Nociari, M. M., W. Telford, and C. Russo. 1999. Post-thymic development of $CD28^-CD8^+$ T cell subset: age-associated expansion and shift from memory to naive phenotype. *J. Immunol.* 162: 3327–3335.
50. Bennett, S. R., F. R. Carbone, F. Karamalis, R. A. Flavell, J. F. Miller, and W. R. Heath. 1998. Help for cytotoxic T cell responses is mediated by CD40 signaling. *Nature* 393: 478–480.
51. Wallace, M. E., R. Keating, W. R. Heath, and F. R. Carbone. 1999. The cytotoxic T cell response to herpes simplex virus type 1 infection of C57BL/6 mice is almost entirely directed against a single immunodominant determinant. *J. Virol.* 73: 7619–7626.
52. Osorio, Y., and H. Ghiasi. 2003. Comparison of adjuvant efficacy of herpes simplex virus type 1 recombinant viruses expressing Th1 and Th2 cytokine genes. *J. Virol.* 77: 5774–5783.
53. Pawelec, G., R. B. Effros, C. Caruso, E. Remarque, Y. Barnett, and R. Solana. 1999. T cells and aging. *Front. Biosci.* 4: 216–269.
54. Wilcoxen, S. C., E. Kirkman, K. C. Dowdell, and S. A. Stohlman. 2000. Gender-dependent IL-12 secretion by APC is regulated by IL-10. *J. Immunol.* 164: 6237–6243.
55. Benten, W. P., M. Lieberherr, G. Giese, C. Wrehlke, O. Stamm, C. E. Sekeris, H. Mossmann, and F. Wunderlich. 1999. Functional testosterone receptors in plasma membranes of T cells. *FASEB J.* 13: 123–133.
56. Haller, G. W., N. Esnaola, K. Yamada, A. Wu, A. Shimizu, A. Hansen, V. R. Ferrara, K. S. Allison, R. B. Colvin, M. Sykes, and D. H. Sachs. 1999. Thymic transplantation across an MHC class I barrier in Swine. *J. Immunol.* 163: 3785–3792.
57. Duncan, S. R., N. G. Capetanakis, B. R. Lawson, and A. N. Theofilopoulos. 2002. Thymic dendritic cells traffic to thymi of allogeneic recipients and prolong graft survival. *J. Clin. Invest.* 109: 755–764.
58. Garzetti, G. G., A. Ciavattini, M. Provinciali, M. Muzzioli, G. Di Stefano, and N. Fabris. 1996. Natural cytotoxicity and GnRH agonist administration in advanced endometriosis: positive modulation on natural killer activity. *Obstet. Gynecol.* 88: 234–240.
59. Oliver, R. T. D., J. V. Joseph, and C. J. Gallagher. 1995. Castration-induced lymphocytosis in prostate cancer: possible evidence for gonad/thymus endocrine interaction in man. *Urol. Int.* 54: 226–229.
60. Umesaki, N., T. Tanaka, M. Miyama, K. Mizuno, N. Kawamura, and S. Ogita. 1999. Increased natural killer cell activities in patients treated with gonadotropin releasing hormone agonist. *Gynecol. Obstet. Invest.* 48: 66–68.
61. Jacobson, J. D., and M. A. Ansari. 2004. Immunomodulatory actions of gonadal steroids may be mediated by gonadotropin-releasing hormone. *Endocrinology* 145: 330–336.
62. Batticane, N., M. C. Morale, F. Gallo, Z. Farinella, and B. Marchetti. 1991. Luteinizing hormone-releasing hormone signaling at the lymphocyte involves stimulation of interleukin-2 receptor expression. *Endocrinology* 129: 277–286
63. Marchetti, B., V. Guarcello, M. C. Morale, G. Bartoloni, Z. Farinella, S. Cordaro, and U. Scapagnini. 1989. Luteinizing hormone-releasing hormone-binding sites in the rat thymus: characteristics and biological function. *Endocrinology* 125: 1025–1036.
64. Mercader, M., B. K. Bodner, M. T. Moser, P. S. Kwon, E. S. Park, R. G. Manecke, T. M. Ellis, E. M. Wojcik, D. Yang, R. C. Flanigan, et al. 2001. T cell infiltration of the prostate induced by androgen withdrawal in patients with prostate cancer. *Proc. Natl. Acad. Sci. USA* 98: 14565–14570.
65. Sundaram, K., A. Keizer-Zucker, R. B. Thau, and C. W. Bardin. 1987. Reversal of testicular function after prolonged suppression with an LHRH agonist in rhesus monkeys. *J. Androl.* 8: 103–107.